Electronic Supplementary Information

Self-assembled mononuclear complexes: open metal sites and inverse dimension-dependent catalytic activity for Knoevenagel condensation and CO₂ cycloaddition

Heng Xu, [1] Lexi Zhang, [*1] Yue Xing, [1] Yanyan Yin, [*2] Bo Tang [1] and Lijian Bie [*1]

[1] School of Materials Science and Engineering, Tianjin Key Lab for Photoelectric Materials and Devices, Key Laboratory of Display Materials and Photoelectric Devices (Ministry of Education), National Demonstration Center for Experimental Function Materials Education, Tianjin University of Technology, Tianjin 300384, China

[2] Department of Environmental Science and Engineering, Nankai University Binhai College, Tianjin 300270, China

[*] Corresponding authors:

Le-Xi Zhang, Tel./Fax: +86 022 60214028. E–Mail: lxzhang@tjut.edu.cn

Yan-Yan Yin, Tel./Fax: +86 022 63304761. E–Mail: yinyanyanyyyy@163.com

Li-Jian Bie, Tel./Fax: +86 022 60215508. E–Mail: ljbie@tjut.edu.cn

Contents

S1. Experimental section

S1.1. Materials

All the solvents and reagents were purchased from commercial sources and used without further purification.

S1.2. Analytical methods

The single-crystal X-ray diffraction (SXRD) data were collected at room temperature (RT) on a XtaLAB PRO diffractometer with graphite-monochromated Cu Kα radiation (λ = 1.5406 Å) (Rigaku, Japan). Diffraction intensities were collected with a CCD area detector image plate diffractometer by using the ω/φ scan technique. Absorption corrections were applied by using multiscan techniques. The structures were solved by direct methods with SHELXS and refined by least-squares procedures on F_o^2 using SHELXL by minimizing the function $\Sigma_\omega(F_o^2-F_c^2)^2$ in the Olex2 package, where F_o and F_c are the observed and calculated structure factors, respectively. All non-hydrogen atoms were located geometrically and refined with anisotropic temperature parameters; hydrogen atoms were refined as rigid groups. The powder X-ray diffraction (PXRD) patterns were collected from 8° to 55°, with a step of 0.02° and data collection time of 0.2 s, on a Rigaku D/max-2500 advance diffractometer (Rigaku, Japan) with Cu-Kα1 radiation (λ = 1.54056 Å). Elemental analyses (C, H, and N) were carried on a Vario EL Cube elemental analyzer (Elementar, German). Pictures and videos of the microscope were obtained from Modle BX53MTRF-S (Olympus, Japan) and DFM-40C (Caikon, China), respectively. Thermogravimetric analysis (TGA) was obtained

with a mass of around 5.0 mg, in the temperature range from RT to 700 °C using TA Instruments TG/DTA 6300 in N_2 with a heating rate of 10 °C min^{-1}. The specific surface areas were measured via the Brunauer-Emmett-Teller (BET) method using N_2 adsorption at 77 K after treating the samples at 60 °C and 10^{-4} Pa for 2 h using BELSORP-max (MicrotracBEL, Japan). The Fourier Transform infrared (FT-IR) spectra were recorded on a Nicolet iS10 spectrometer with KBr pellets in the range of 4000–700 cm^{-1} (Thermo Fisher Scientific, USA). All catalytic experiments were performed using a WP-TEC-1020HSL reactor from Xi'an WATTCAS Chemical Technology Co. Ltd, China. The compounds were performed on Agilent 7890B/5977B by injection in a gas chromatograph coupled with a mass spectrometer (GC-MS) using a silica column of HP-5 (30 × 0.25 × 0.25).

S1.3. Synthesis and structural characterization of catalysts

Preparation of [Cu(TMA)(2,2'-bpy)H_2O]·2H_2O (**1**): 1 mmol Cu(OAc)$_2$·H_2O, 1 mmol TMA, and 1 mmol bpy were completely dissolved in 30 mL deionized water and 30 mL ethanol under magnetic stirring for 15 min. The mixture was filtered and the clear solution was kept stand still without any disturbance at r.t. Sapphire transparent plate-shaped crystals were finally obtained through slow evaporation of the filtered solution in air for 12 h. The experimental procedure can be repeated easily with an average yield of ca. 52% based on Cu^{2+}. Elemental analysis (%) calculated for ($C_{17}H_{18}CuN_2O_5S$) (**1**): C, 47.94; H, 4.26; N, 6.58. Found (**1**): C, 47.93; H, 4.27; N, 6.56. FT-IR (KBr, cm^{-1}): 3416 (vs), 3113 (m), 2944 (w), 1640 (vs), 1597 (vs), 1495 (w), 1447 (s), 1408 (vs),

1313 (m), 1252 (w), 1156 (w), 976 (w), 964 (w), 818 (m), 772 (s), 732 (m).

Preparation of [Cu(TMA)(phen)H$_2$O]·2H$_2$O (**2**): 1 mmol Cu(OAc)$_2$·H$_2$O, 1 mmol TMA, and 1 mmol phen were completely dissolved in 30mL deionized water and 30 mL ethanol under magnetic stirring for 20 min. The resulting grey blue product was filtered off. Grey blue transparent lump crystals were finally obtained through slow evaporation of the filtered solution in air for 2 days. The experimental procedure can be repeated easily with an average yield of ca. 48% based on Cu^{2+}. Elemental analysis (%) calculated for (C$_{19}$H$_{18}$CuN$_2$O$_7$S) (**1**): C, 47.35; H, 3.76; N, 5.81. Found (**1**): C, 47.33; H, 3.78; N, 5.79. FT-IR (KBr, cm^{-1}): 3440 (vs), 3119 (m), 2944 (w), 1632 (vs), 1582 (vs), 1519 (w), 1428 (m), 1404 (vs), 1343 (w), 1223 (w), 1197 (w), 976 (w), 962 (w), 874 (w), 852 (m), 747 (m), 724 (s).

Preparation of [Cu(TMA)(3-CNPy)] (**3**): 1 mmol Cu(OAc)$_2$·H$_2$O, 1 mmol TMA, and 1 mmol 3-CNPy were completely dissolved in 30 mL deionized water and 30 mL ethanol under magnetic stirring for 10 min. The generated precipitate was separated by filtration. Azure transparent needle-like crystals were finally obtained through slow evaporation of the filtered solution in air for 3 days. The experimental procedure can be repeated easily with an average yield of ca. 61% based on Cu^{2+}. Elemental analysis (%) calculated for (C$_{13}$H$_8$CuN$_2$O$_4$S) (**1**): C, 44.38; H, 2.29; N, 7.96. Found (**1**): C, 44.39; H, 2.31; N, 7.95. FT-IR (KBr, cm^{-1}): 3440 (vs), 3103 (w), 2920 (w), 2235 (w), 1680 (vs), 1595 (vs), 1564 (vs), 1474 (w), 1419(m), 1335 (s), 1242 (w), 1181 (w), 964 (w), 923 (w), 835 (w), 757 (s).

Preparation of [Zn(TMA)(2,2'-bpy)H$_2$O]·2H$_2$O (**4**): 1 mmol Zn(OAc)$_2$·2H$_2$O, 1 mmol TMA, and 1 mmol bpy were completely dissolved in 20 mL deionized water and 30 mL ethanol under magnetic stirring for 15 min. The mixture was filtered and the clear solution was kept stand still without any disturbance at r.t. Transparent schistose crystals were finally obtained through slow evaporation of the filtered solution in air for 3 days. The experimental procedure can be repeated easily with an average yield of ca. 47% based on Zn^{2+}. Elemental analysis (%) calculated for (C$_{17}$H$_{18}$ZnN$_2$O$_5$S) (**1**): C, 42.73; H, 4.22; N, 5.86. Found (**1**): C, 42.74; H, 4.24; N, 5.85. FT-IR (KBr, cm^{-1}): 3424 (vs), 3078 (m), 2924 (w), 1602 (vs), 1598 (vs), 1492 (w), 1444 (s), 1418 (m), 1337 (m), 1317 (m), 1156 (w), 1027 (w), 967 (w), 819 (w), 769 (vs), 736 (m).

S1.4. Thermal stability

The thermal stability of the synthesized samples was assessed by thermogravimetric analysis (TGA) by heating the complexes **1-4** from RT to 700 °C under a N$_2$ atmosphere.

S1.5 DFT calculation

The DFT calculation was performed by using the Dmol^3 code.[1] The exchange and correlation energies were determined with the Perdew, Burke, and Ernzerhof (PBE) functional within the generalized gradient approximation (GGA).[2] The DFT semi-core pseudo potentials (DSPPs) core treatment is implemented for relativistic effects, which replaces core electrons by a single effective potential and introduces some degree of relativistic correction into the core.[3] Moreover, the double numerical plus polarization (DNP) is chosen as the basis set. A thermal smearing of 0.005 Ha (1 Ha = 27.21 eV) to

the orbital occupation is applied to speed up electronic convergence. The convergence tolerance of energy, maximum force, and maximum displacement for geometry optimization are 1×10^{-5} Ha, 0.002 Ha/Å, and 0.005 Å, respectively. The transition states (TS) for HCOOH decomposition are obtained by LST/QST tools in Dmol[3] code. The root-mean-square (RMS) convergence for TS search is set to be 0.002 Ha/Å. Stretching frequencies are analyzed to characterize the transition states, for which only one imaginary frequency of each of them was found.[4]

S2. Catalysis Experiments

S2.1. Knoevenagel condensation reaction

S2.1.1. Typical procedure

A schlenk reaction tube was charged with benzaldehyde (1.0 mmol), malononitrile (1.3 mmol) and catalyst (0.5 mol%). The mixture was stirred at r.t for 1 h. When the reaction was completed, the catalyst was recovered by centrifugation. Then the catalyst was filtered off, washed with ethanol and water, dried, and reused without further purification and regeneration. Moreover, the recovered catalysts were characterized by powder X-ray diffraction (PXRD) and showed identical results to those of the fresh samples. Gas chromatograph coupled with a mass spectrometer (GC-MS) was used to detect the catalytic effect of the reaction qualitatively and quantitatively.

S2.1.2. Ultrasonic procedure

To a 1.5 mL centrifuge tube, benzaldehyde (1.0 mmol), malononitrile (1.3 mmol) and catalyst (2 mol%) were added under ambient conditions. The tube was immersed in the ultrasonic bath in an open atmosphere for up to 30 min. Then, an appropriate amount of acetonitrile was added to remove the catalyst by centrifugation. The liquid was transferred to a 25 mL volumetric flask and mixed with acetonitrile. The mixture was stirred, then a sample (1.5 mL) was removed from the organic phase and analyzed by GC-MS.

S2.2. CO$_2$-epoxide cycloaddition reaction

All the cycloaddition reactions were conducted in a 20 mL schlenk reaction tube

charged with the requisite amount of catalyst, epoxide, and cocatalyst under magnetic stirring at 800 rpm. The reactions were conducted under 1 atm CO_2 pressures at different temperatures. The yields were then determined using a GC-MS.

S3. Fig. S1-S9 and Tab.S1-S9
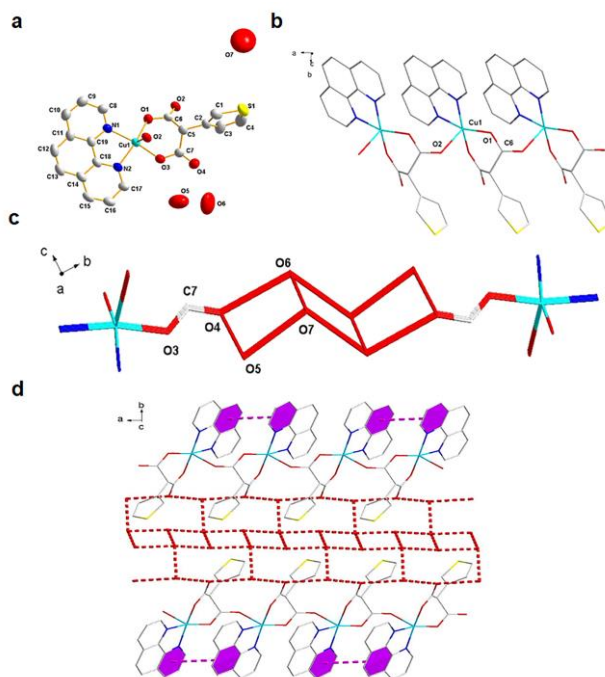
Fig. S1. a) Coordination environments of Cu^{2+} site in **2**; b) Cu^{2+} site connected by TMA^{2-} anions; c) The adjacent Cu^{2+} sites are linked together along *bc* plane by indirect hydrogen interactions; d) On the *ab* plane, 2D supramolecular layer links with another equivalent layer through indirect hydrogen bonds and π···π interactions to form 2D supramolecular bilayer.
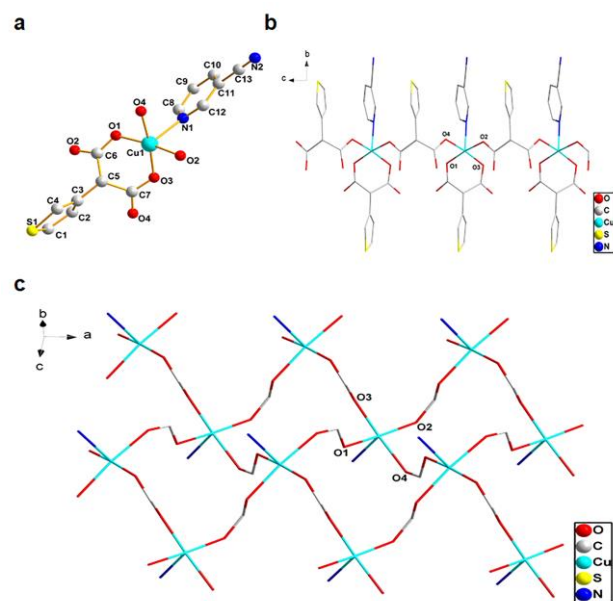
Fig. S2. a) View of the coordination environment of the Cu^{2+} cation in **3**; b) Cu^{2+} sites connected by TMA^{2-} anions; c) 2D structure of **3** stabilized by carboxylate radical (O1, O2, O3 and O4).
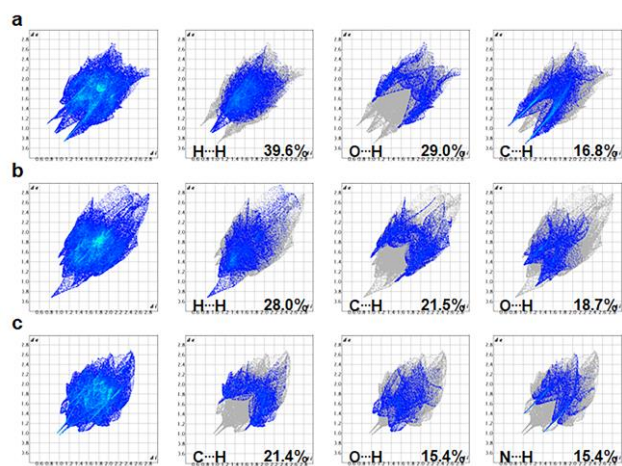
Fig. S3. All and decomposed FP plots (a-c), presenting percentage contribution of the following intermolecular contacts to the total Hirshfeld surface area: total, H···H, O···H, C···H or N···H of **1, 2** and **3** crystal structures.
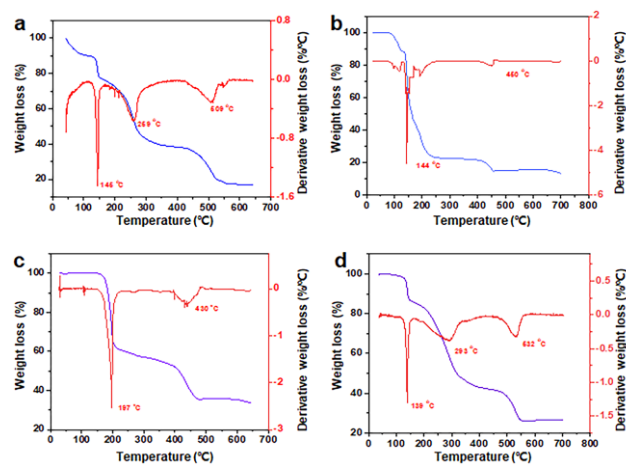
Fig. S4. TGA plots of complexes a) **1**, b) **2** c) **3**, and d) **4**, respectively.
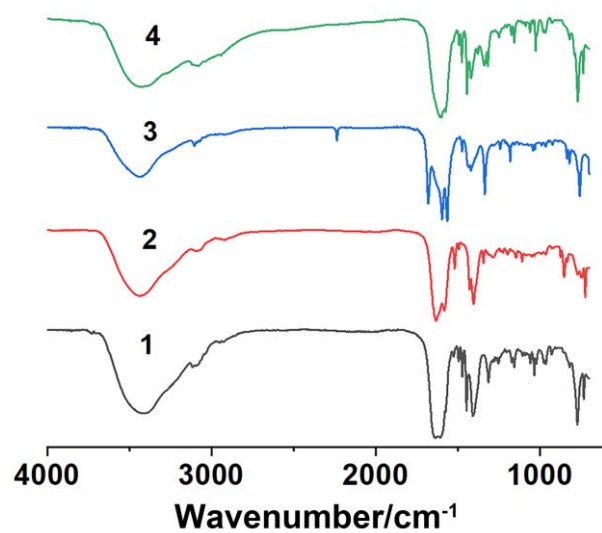
Fig. S5. FT-IR spectra of complexes **1**-**4**, respectively.
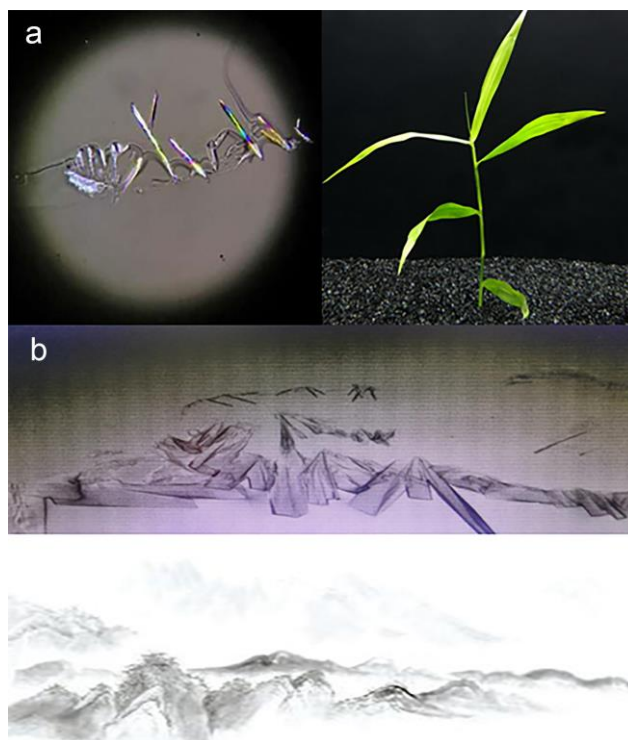
Fig. S6. The photos of complex **1** crystallized for a) 5 min and b) 30 min, respectively.
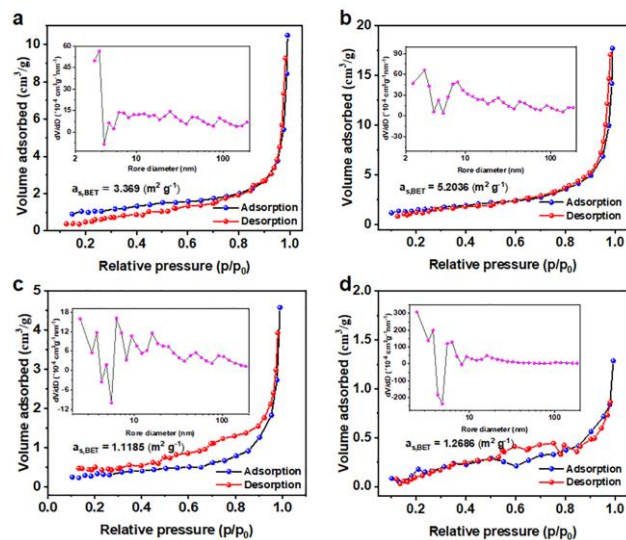
Fig. S7. N_2 adsorption of complexes a) **1**, b) **2**, c) **3**, and d) **4**, respectively.
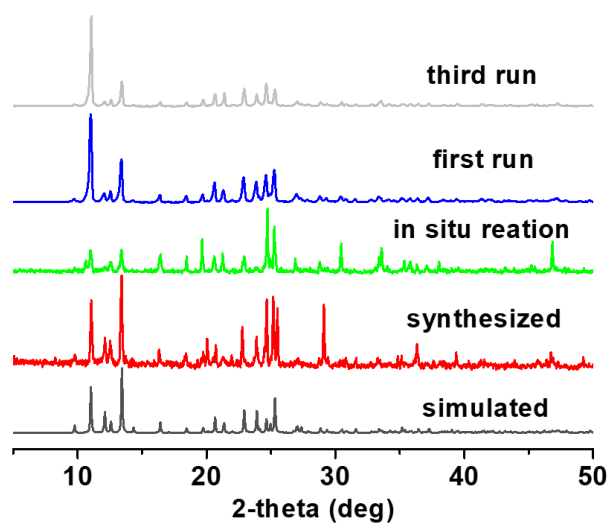
Fig. S8. The PXRD patterns of complex **4**. Black: XRD simulated with cif. Red: XRD obtained by culturing out the crystals. Green: XRD of solids produced during in situ catalytic reactions. Blue: XRD of catalyst after one cycle reaction. Grey: XRD of catalyst after five cycles of reaction.
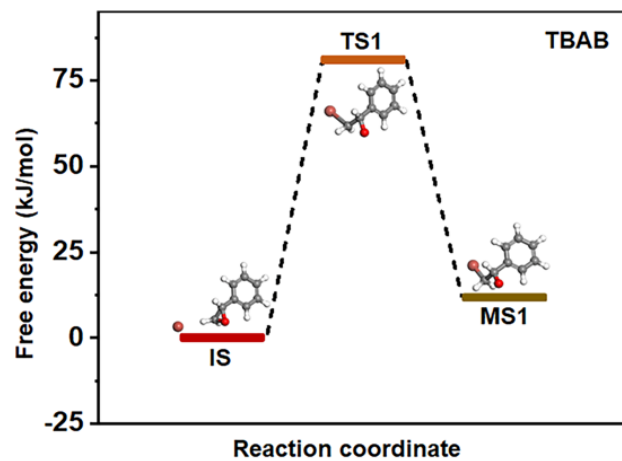
Fig. S9. Free energy profiles for the TBAB catalyzed ring opening.

Tab. S1. X-ray crystallographic data and structural refinement for **1-4**.

Complex	1	2	3	4
Formula	$C_{17}H_{18}CuN_2O_5S$	$C_{19}H_{18}CuN_2O_7S$	$C_{13}H_8CuN_2O_4S$	$C_{17}H_{18}ZnN_2O_5S$
Mr	457.93	481.95	351.81	459.76
Temperature	293 K	293 K	293 K	293 K
Crystal system	Orthorhombic	Monoclinic	Monoclinic	Orthorhombic
Space group	*Pbca*	*P21/n*	*P21/n*	*Pbca*
a(Å)	16.10966 (19)	4.9913 (2)	6.17103(14)	16.0233(3)
b(Å)	14.61582 (19)	26.3098 (11)	31.0014(7)	14.6001(2)
c(Å)	16.4897 (2)	14.5516 (6)	6.95964(16)	16.6104(3)
α(deg)	90	90	90	90
β(deg)	90	95.274 (4)	93.726(2)	90
γ(deg)	90	90	90	90
V(Å^3)	3882.59(8)	1902.83(14)	1328.64(5)	3885.86(11)
Z	8	4	4	8
D(Mg·m^{-3})	1.567	1.682	1.759	1.572
F(000)	1880.0	988.0	708.0	1888.0
θ range	4.918 to 78.40°	3.36 to 79.26°	2.85 to 79.12°	4.89 to 79.16°
Limiting indices	$-20 \leq h \leq 20$, $-18 \leq k \leq 15$, $-17 \leq l \leq 20$	$-6 \leq h \leq 6$, $-33 \leq k \leq 29$, $-16 \leq l \leq 18$	$-7 \leq h \leq 7$, $-38 \leq k \leq 37$, $-8 \leq l \leq 8$	$-20 \leq h \leq 16$, $-9 \leq k \leq 18$, $-21 \leq l \leq 18$
CCDC No.	2130947	2131195	2130946	2131194

Selected Bond Distances (Å) and Angles (°) for **1-4**.

1

Cu(1)-O(3)	1.941(3)	Cu(1)-N(2)	2.006(4)
Cu(1)-O(1)	1.954(4)	Cu(1)-O(5)	2.153(4)
Cu(1)-N(1)	1.995(4)		
O(3)-Cu(1)-O(1)	90.26(15)	N(1)-Cu(1)-N(2)	80.64(17)
O(3)-Cu(1)-N(1)	167.34(17)	O(3)-Cu(1)-O(5)	97.92(16)
O(1)-Cu(1)-N(1)	92.70(16)	O(1)-Cu(1)-O(5)	97.83(17)
O(3)-Cu(1)-N(2)	92.25(17)	N(1)-Cu(1)-O(5)	93.86(17)
O(1)-Cu(1)-N(2)	158.88(18)	N(2)-Cu(1)-O(5)	102.57(18)

2

Cu(1)-O(3)	1.915(3)	Cu(1)-N(1)	2.001(4)
Cu(1)-O(1)	1.934(3)	Cu(1)-N(2)	2.020(4)
Cu(1)-O(2)#2	2.316(3)		
O(3)-Cu(1)-O(1)	92.68(13)	N(1)-Cu(1)-N(2)	82.06(15)
O(3)-Cu(1)-N(1)	169.14(15)	O(3)-Cu(1)-O(2)#2	92.81(14)
O(1)-Cu(1)-N(1)	91.47(14)	O(1)-Cu(1)-O(2)#2	100.94(13)
O(3)-Cu(1)-N(2)	91.12(14)	N(1)-Cu(1)-O(2)#2	96.26(14)
O(1)-Cu(1)-N(2)	162.77(15)	N(2)-Cu(1)-O(2)#2	95.65(13)

Symmetry transformations used to generate equivalent atoms: #2 x+1, y, z

3

Cu(1)-O(1)	1.947(6)	Cu(1)-O(3)	1.992(6)
Cu(1)-O(21)	1.992(5)	Cu(1)-O(42)	2.003(6)
Cu(1)-N(1)	2.256(7)		
O(1)-Cu(1)-O(21)	173.1(2)	O(1)-Cu(1)-O(42)	89.2(3)
O(21)-Cu(1)-O(42)	93.3(2)	O(1)-Cu(1)-O(3)	88.7(2)
O(21)-Cu(1)-O(3)	88.0(2)	O(42)-Cu(1)-O(3)	172.6(2)
O(1)-Cu(1)-N(1)	100.5(3)	O(21)-Cu(1)-N(1)	85.9(3)

O(42)-Cu(1)-N(1)	89.7(3)	O(3)-Cu(1)-N(1)	97.6(3)

4

Zn(1)-O(5)	1.968(4)	Zn(1)-O(4)	2.006(4)
Zn(1)-O(2)	2.031(3)	Zn(1)-N(13)	2.107(4)
Zn(1)-N(7)	2.124(4)		
O(5)-Zn(1)-O(4)	104.68(17)	O(2)-Zn(1)-N(13)	89.67(16)
O(5)-Zn(1)-O(2)	101.52(15)	O(5)-Zn(1)-N(7)	101.56(17)
O(4)-Zn(1)-O(2)	88.89(14)	O(4)-Zn(1)-N(7)	90.76(15)
O(5)-Zn(1)-N(13)	110.24(18)	O(2)-Zn(1)-N(7)	156.22(16)
O(4)-Zn(1)-N(13)	144.61(17)	N(13)-Zn(1)-N(7)	77.03(17)

Tab. S2. Contributions (%) of main interactions to the FP plots for **1-3**.

Various interactions	1	2	3
H···H	39.6	28.0	15.1
O···H	29.0	18.7	15.4
C···H	16.8	21.5	21.4
S···H	5.2	9.1	6.0
C···C	3	2.7	2.4
S···O	2.5	trace	0.7
N···H	1.8	1.5	15.4
O···O	trace	2.0	5.1
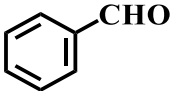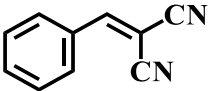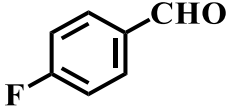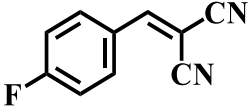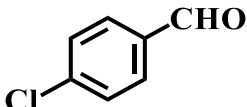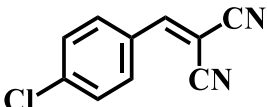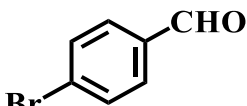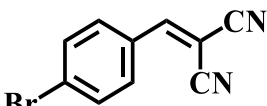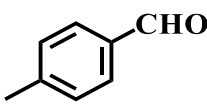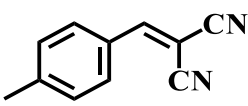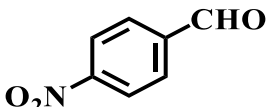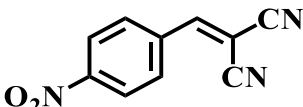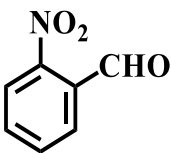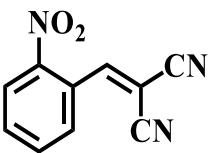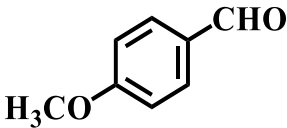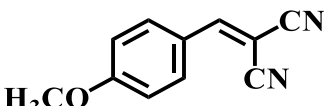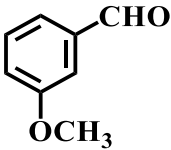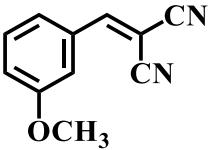
Tab. S3. Screening of catalysts.
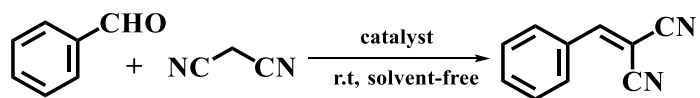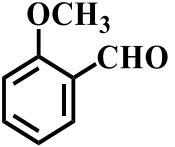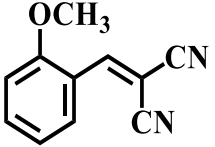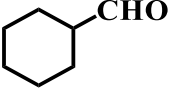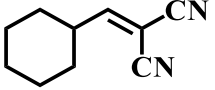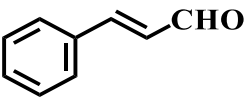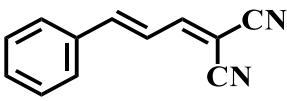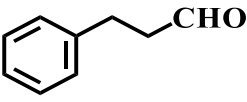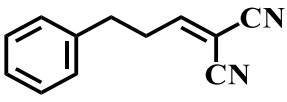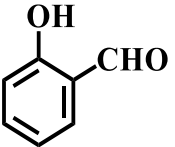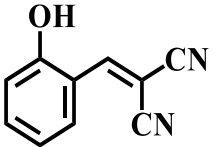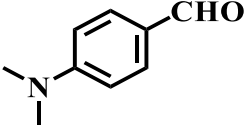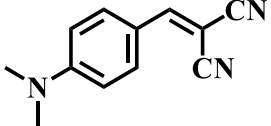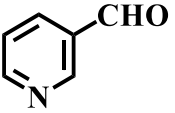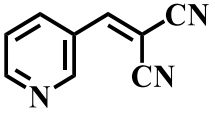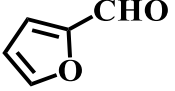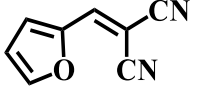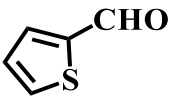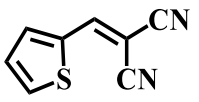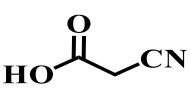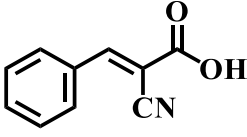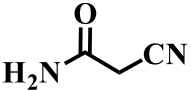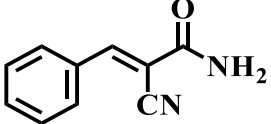
Empirical	Catalyst	Yield (%) [a]	Sele (%)
1	-	Trace	
2	Cu(Ac)$_2$·2H$_2$O + bpy	100	100
3	Cu(Ac)$_2$·2H$_2$O + phen	95.30	100
4	Cu(Ac)$_2$·2H$_2$O + 3-CNPy	34.18	100
5	**1**	100	100
6	**2**	95.46	100
7	**3**	35.25	100
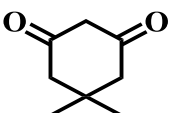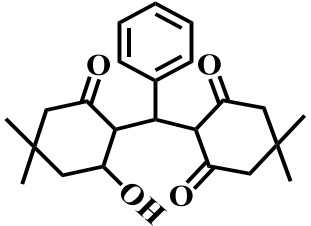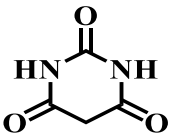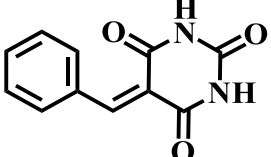
Reaction conditions: malononitrile (1.3 mmol), benzaldehyde (1.0 mmol), catalyst (0.5 mol%), 30 min, ultrasound (200 W).

[a] Yields of products were determined by GC-MS.

Tab. S4. Evaluation of the catalytic activity of complex **1** for Knoevenagel condensation. [a]

Entry	Reactant	Product	Yield (%) [b]
1			100
2			95.97
3			60.79
4			32.50
5			96.65
6			100
7			82.23
8			84.85
9			51.95

#	Substrate	Product	Yield
10	2-methoxybenzaldehyde (OCH₃, CHO)	2-(2-methoxybenzylidene)malononitrile (CN, CN)	65.06
11	cyclohexanecarbaldehyde (CHO)	2-(cyclohexylmethylene)malononitrile (CN, CN)	83.51
12	cinnamaldehyde (CHO)	(CN, CN)	30.31
13	3-phenylpropanal (CHO)	(CN, CN)	54.87
14	salicylaldehyde (OH, CHO)	(CN, CN)	45.32
15	4-(dimethylamino)benzaldehyde (N, CHO)	(CN, CN)	trace
16	nicotinaldehyde (pyridine, CHO)	(CN, CN)	100
17	furfural (O, CHO)	(CN, CN)	80.48
18	thiophene-2-carbaldehyde (S, CHO)	(CN, CN)	92.61
19	cyanoacetic acid (HO, O, CN)	(O, OH, CN)	85.06
20	2-cyanoacetamide (H₂N, O, CN)	(O, NH₂, CN)	100

| 21 | | | 74.84 |
| 22 | | | 90.14 |

[a] Reaction conditions: entry 1-18: 1.0 mmol reactant, 1.3 mmol malononitrile; entry

19-22: 1.0 mmol reactant, 1.3 mmol benzaldehyde, r.t, 60 min, 0.5 mol% catalyst **1**.

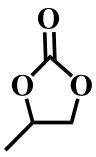[b] Catalytic reaction products were analyzed and identified by GC–MS.
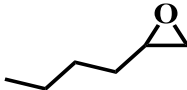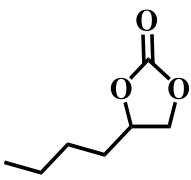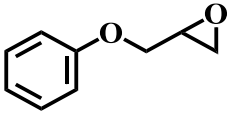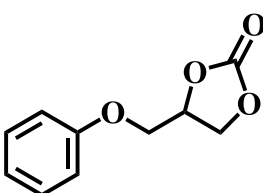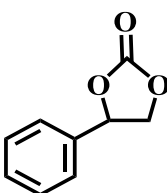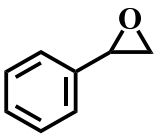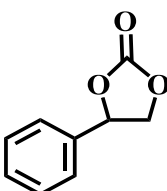
Tab. S5. Free energy of the optimized structures of the Knoevenagel condensation reaction pathway catalyzed by complex **1**.

	IS	TS1	MS1	MS2	TS2	MS3	TS3	MS4	TS
Free energy (KJ/mol)	0	43.6	-13.2	-56.9	7.6	-53.8	19.4	-53.9	-14.7

Tab. S6. Comparison with different MOF catalysts in the cyclic addition of CO_2 and epoxides.

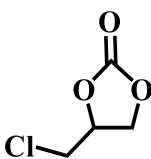| entry	Catalyst	Yield (%)	P / Mpa	T / °C	T / h	References
1	**4**	100	0.1	r.t	19.5	this work
2	Ni–TCPE1	>99	1	100	12	5
3	$[Cu_4(L_1)]_n$	96	0.1	r.t	48	6
4	FJI-H14	86	0.1	80	24	7
5	VPI-100	96	1	90	6	8
6	V8-1	>99	0.5	70	16	9
7	HE-ZIF-BM	97	1	100	10	10
8	MOF@mSiO_2-YS	91	0.8	r.t	48	11
9	CuBDC/CMC	91.5	0.1	80	17	12

Tab. S7. Cycloaddition of CO_2 with various epoxides.[a]

Entry	Reactant	Product	Yield (%) [b]
1			100
2			95.97
3			60.79
4			32.50
5 [c]			96.65
6 [d]			100

[a] Reaction conditions: substrate (2.0 mmol), CO_2 (1 atm), TBAB (15 mg), 0.25 mol% catalyst **4**, solvent-free, r.t, 19.5 h.

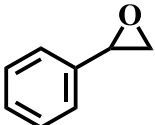[b] Yields of products were determined by GC-MS. [c] Bu$_4$NCl replace of TBAB. [d] Bu$_4$NI replace of TBAB.

Tab. S8. Free energy of the optimized structures of the CO_2 cycloaddition reaction pathway catalyzed by complexes **1** and **4**.

1

	IS	TS1	MS1	MS2	TS2	MS3	TS3	MS4	TS
Free energy (KJ/mol)	0	65.2	-17.8	-14.8	-14.86	-10.1	22.4	-74.2	-49.4

4

	IS	TS1	MS1	MS2	TS2	MS3	TS3	MS4	TS
Free energy (KJ/mol)	0	35.5	-24.6	-14.8	-14.86	-10.1	22.4	-74.2	-49.4

Tab. S9. Free energy profiles for the TBAB catalyzed ring opening calculated.

	IS	TS1	MS1
Free energy (KJ/mol)	0	80.9	11.6

References

1. B. Delley, *J. Chem. Phys.*, 2000, **113**, 7756–7764.

2. J. P. Perdew, K. Burke and M. Ernzerhof, *Phys. Rev. Lett.*, 1996, **77**, 3865.

3. B. Delley, *Phys. Rev. B*, 2002, **66**, 155125.

4. D. Sheppard, R. Terrell and G. Henkelman, *J. Chem. Phys.*, 2008, **128**, 134106.

5. Z. Zhou, C. He, J. Xiu, L. Yang and C.-Y. Duan, *J. Am. Chem. Soc.*, 2015, **137**, 15066–15069.

6. P.-Z. Li, X.-J. Wang, J. Liu, J.-S. Lim, R.-Q. Zou and Y.-L. Zhao, *J. Am. Chem. Soc.*, 2016 **138**, 2142–2145.

7. L.-F. Liang, C.-P. Liu, F.-L. Jiang, Q.-H. Chen, L.-J. Zhang, H. Xue, H.-L. Jiang, J.-J. Qian, D.-Q. Yuan and M.-C. Hong, *Nat. Commun.*, 2017, **8**, 1–10.

8. J. Zhu, P. M. Usov, W.-Q. Xu, P. J. Celis-Salazar, S.-Y. Lin, M. C. Kessinger, C. Landaverde-Alvarado, M. Cai, A. M. May, C. Slebodnick, D.-R. Zhu, S. D. Senanayake and A. J. Morris, *J. Am. Chem. Soc.*, 2018, **140**, 993–1003.

9. J.-P. Cao, Y.-S. Xue, N.-F. Li, J.-J. Gong, R.-K. Kang and Y. Xu, *J. Am. Chem. Soc.*, 2019, **141**, 19487–19497.

10. W. Xu, H. Chen, K.-C. Jie, Z.-Z. Yang, T.-T. Li and S. Dai, *Angew. Chem.*, 2019, **131**, 5072–5076.

11. S.-X. Bao, J.-Y. Li, B.-Y. Guan, M.-J. Jia, O. Terasaki and J.-H. Yu, *Matter*, 2020, **3**, 498–508.

12. X.-Y. Bai, X.-Y. Lu, R. Ju, H. Chen, L. Shao, X. Zhai, Y.-N. Li, F.-Q. Fan, Y. Fu

and W. Qi, *Angew. Chem., Int. Ed.*, 2021, **60**, 701–705.